

<https://doi.org/10.1038/s43247-024-01693-0>

Decline in Atlantic Niño prediction skill in the North American multi-model ensemble

Yihao Chen^{1,2}, Xiaoqin Yan^{1,2}✉, Youmin Tang^{1,2,3}✉, Qingyang Song^{1,2}, Zheqi Shen^{1,2} & Yanling Wu^{1,2}

The Atlantic Niño has attracted considerable attention due to its profound climatic impacts. It has been reported that the strength of Atlantic Niño has been weakening since 2000, but it is not clear whether it would lead to a change in Atlantic Niño prediction skill. Here we find a dramatic decline in Atlantic Niño prediction skill since 2000 by evaluating the predictions of the North American Multi-Model Ensemble. The prediction skill decline is mainly associated with a climatic regime shift, which leads to a weakened El Niño–Southern Oscillation (ENSO) teleconnection to the sea surface temperature anomaly dipole mode over the South Atlantic. A systematic model deficiency may amplify the prediction skill decline. This study offers insights for understanding the Atlantic Niño predictability and for improving the simulation and prediction of Atlantic Niño events.

The Atlantic Niño has attracted considerable attention from the climate community^{1–4}, as it comprises the dominant source of interannual climate variability in the tropical Atlantic region^{5,6} and serves as a potential precursor of El Niño–Southern Oscillation (ENSO)^{7–12}.

The Atlantic Niño could be driven by multiple mechanisms^{13–15}. For example, Bjerknes feedback is considered as the fundamental mechanism of Atlantic Niño^{5,16}. Thermodynamic processes are also suggested to be non-negligible for the Atlantic Niño^{17,18}. Perturbations across the off-equatorial areas of the Atlantic Ocean^{19–22} and the tropical Indian Ocean²³ can trigger the Atlantic Niño as well. In particular, the South Atlantic Ocean Dipole (SAOD), which is a southwest–northeast oriented dipole of sea surface temperature anomalies (SSTA) in the South Atlantic, is found to be closely related to the appearance of Atlantic Niño events^{24,25}.

The Atlantic Niño predictability is relatively less studied. The prediction of Atlantic Niño remains challenging and unsatisfactory^{26–30}. For example, the skillful prediction is restricted to only approximately 4-month lead³¹ using the North American Multi-Model Ensemble (NMME)^{32,33}. Model predictions only capture the evolution of some extremely strong Atlantic Niño events at a 1-month lead³⁴. In addition, it was shown that models with a stronger connection between the boreal autumn Indian Ocean Dipole and the following winter Atlantic Niño appear to have a higher Atlantic Niño prediction skill³⁵. All these studies examined the prediction skill over a fixed length of time period and did not investigate the variation of prediction skill over a long period of time.

Recently, it has been revealed that the Atlantic Niño variability has significantly declined (~30%) during 2000–2017, in comparison with that

during 1982–1999, which could be caused by a weaker Bjerknes feedback and stronger latent heat flux damping³⁶. Additionally, the Atlantic Niño variability was projected to be suppressed under the global warming impacts^{37,38}. Although 2019 and 2021 experienced the resurgence of strong events^{39,40}, it is still interesting and important to examine whether there would be a change in the Atlantic Niño prediction skill given the weakened Atlantic Niño variability, and what could be driving it.

Based on above considerations, we examine the changes in Atlantic Niño prediction skill by evaluating the NMME predictions over two time periods (1982–2000 and 2000–2018). More importantly, potential sources responsible for the changed prediction skill are explored.

Results and discussion

Decline in Atlantic Niño variability and prediction skill

The Atlantic Niño is represented using the ATL3 index⁴¹. Its variability and prediction skill are shown in Fig. 1. The 15-year sliding ATL3 STDs calculated separately from HadISST⁴² and ERSST.v5⁴³ datasets both show a decrease in ATL3 magnitude since 2000, which is consistent with the previous study³⁶. Figure 1b displays the prediction skills of the multiple-model ensemble mean (MME) over the two subperiods. The MME anomaly correlation coefficients (ACCs) at all lead times are significantly lower over the second subperiod, supported by a bootstrap test with resampling times of 10000. The MME ACC decreases ~0.1 at the 0-month lead and ~0.3 at the 5-month lead. At the 2-month lead, the MME decreases most significantly by 38% from 0.74 to 0.46. Although the decrease in prediction skill is consistent with the decrease in variability, the former may not necessarily be

¹Key Laboratory of Marine Hazards Forecasting, Ministry of Natural Resources, Hohai University, Nanjing, China. ²College of Oceanography, Hohai University, Nanjing, China. ³Environmental Science and Engineering, University of North British Columbia, Prince George, BC, Canada. ✉e-mail: xyan@hhu.edu.cn; ytang@unbc.ca

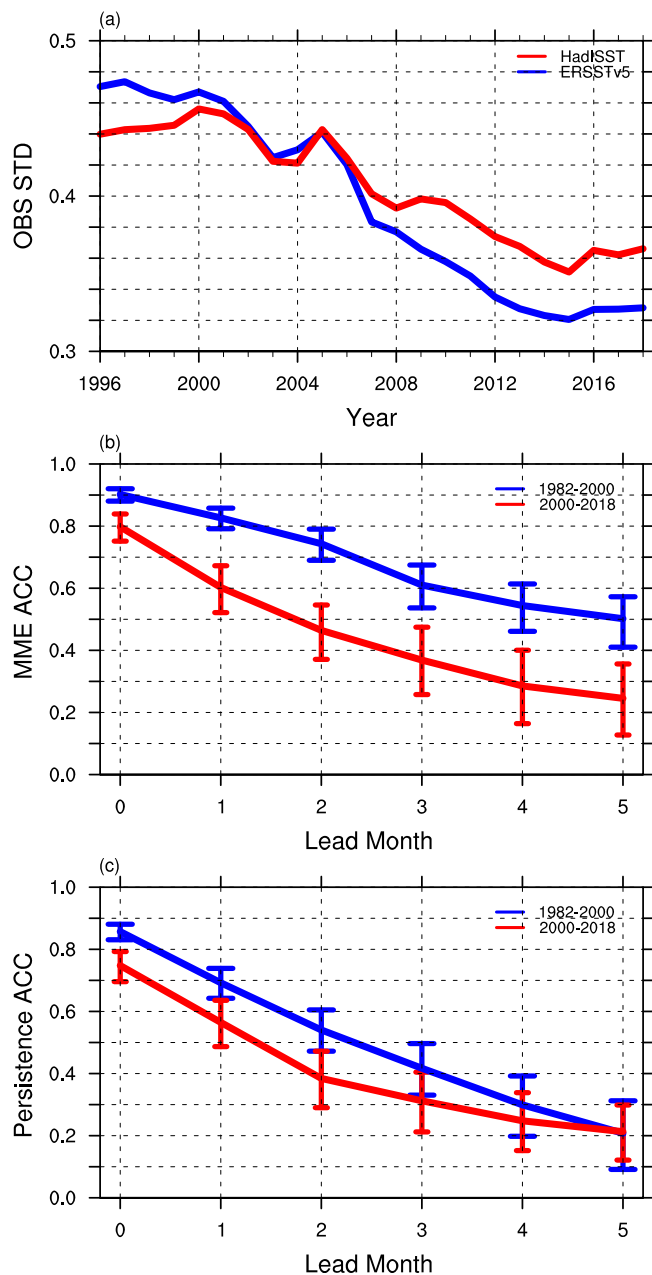


Fig. 1 | The Atlantic Niño variability and prediction skill. **a** 15-year sliding standard deviations (STD) of ATL3 index calculated separately with the HadISST and ERSSTv5 datasets. **b** ACCs of the multiple-model ensemble mean (MME) over the two subperiods. **c** Persistence prediction skills over the two subperiods. The x-axis of (a) indicates the last year of each 15-year sliding window. Error bars in (b) and (c) indicate the 95% confidence interval determined by a bootstrap test with resampling times of 10000.

driven by the latter. Scatter plots of ATL3 prediction skills against ATL3 variabilities (Supplementary Fig. 1) suggest that the Atlantic Niño prediction skill decline has no clear linear relationship with the weakened variability.

Figure 1c shows that the persistence prediction skill declines over the second subperiod as well, indicating a decrease in predictability. However, the persistence prediction skill decreases significantly only at the short leads and does not even change at the 5-month lead. Sliding ACCs of MME and persistence at different lead times, and their difference (Supplementary Fig. 2) confirm that the MME prediction skill decreases more significantly over the second subperiod and that there is an inconsistency between the changes in the MME prediction skill and persistence. As a result, the MME

and persistence prediction skills become comparable at the end of the examined time period (Supplementary Fig. 2c), meaning the failure of dynamical predictions. All these results imply that the significant decline in Atlantic Niño prediction skill in the NMME may relate not only to predictability but also to deficiencies in dynamical predictions, which have great impact on prediction skills^{44–46}.

Changing relationship between the global ocean and Atlantic Niño

To investigate the difference between the two subperiods, we focus on the 2-month lead prediction that shows the most pronounced decline (Fig. 1). For convenience, verification data are referred to as OBS unless otherwise noted. The observed and predicted ATL3 index are regressed on the global SSTA over each subperiod, separately for OBS (Fig. 2a, b) and MME (Fig. 2e, f). Pre-2000, the Atlantic Niño in OBS not only shows a strong correlation with the equatorial Atlantic SSTA, but also shows a significant correlation with global SSTAs over regions such as the subtropical Atlantic Ocean, western Pacific, and eastern Indian Ocean (Fig. 2a). This regression pattern exhibits an inter-Pacific–Atlantic SST gradient and zonal wind anomalies over the equatorial Atlantic, favoring the Bjerknes feedback and development of Atlantic Niño^{7,15,47}. Post-2000, the Atlantic Niño is less associated with SSTA in the tropical Atlantic as well as other ocean basins (Fig. 2b). However, the SSTA dipole structure in the South Atlantic seems to be strengthened and the Atlantic Niño is more closely related to the anomalous cyclone in the South Atlantic Ocean (Fig. 2b), which has been revealed to have a robust link to the Atlantic Niño^{21,25,48}. The correlations between the observed ATL3 and SWP (southwest pole of the SAOD) indices are -0.09 and -0.38 over the first and second subperiod, respectively, indicating the enhanced ATL3–SWP relationship over the second subperiod. It has been found that perturbations of the subtropical anticyclone centered at approximately 30°S to be the predominant mechanism linking the southern extra-tropics and equatorial Atlantic variability, and leading to the SAOD. As such, the SAOD may play a role in the prediction skill decline^{24,25}.

Previous studies have noticed the shift of the Atlantic–Pacific connection and explained it via the modulation of low-frequency variability modes^{49–51}. For example, there is a shift from a period of strong Atlantic–Pacific connection to a period of weak Atlantic–Pacific during the 1970s⁷. In the strong connection period, the Walker circulation is strengthened, favoring the development of coupled processes, and leading to a good correlation between ENSO and the Atlantic Niño, and vice versa in the weak connection period⁷. Moreover, the Atlantic Niño resembles the canonical equatorial mode in the strong connection period, while it behaves as a dipolar structure during the weak connection period⁵², notably similar to the SAOD^{24,25}. Figure 2c, d further displays the regression maps of ATL3 against the global sea level pressure and 200 hPa wind speed anomalies, supporting the weakening Atlantic–Pacific connection since 2000, and indicating a diminished Walker circulation^{7,52}. All these facts indicate that a climatic regime shift occurred around 2000 when the connection of Atlantic Niño and global SSTAs switches from strong to weak. The changing relationship between the global ocean and Atlantic Niño may be responsible for the decreased Atlantic Niño predictability and persistence.

The MME prediction at the 2-month lead well reproduces the climatic regime shift. As can be seen in Fig. 2e, f, the connection of Atlantic Niño and global SSTAs switches from strong to weak in the MME as well. However, in contrast to OBS (Fig. 2b), the MME does not show an apparent dipole structure over the South Atlantic post-2000 (Fig. 2f). This could be a model deficiency in the NMME and may explain the inconsistency between prediction skill declines in the MME and persistence, which will be discussed later.

Intrinsic reason responsible for the decline in Atlantic Niño prediction skill

One might intuitively think that the changed ENSO–ATL3 relationship would be responsible for the skill decline. However, no significant correlation is found between the ATL3 prediction skills and ENSO–ATL3

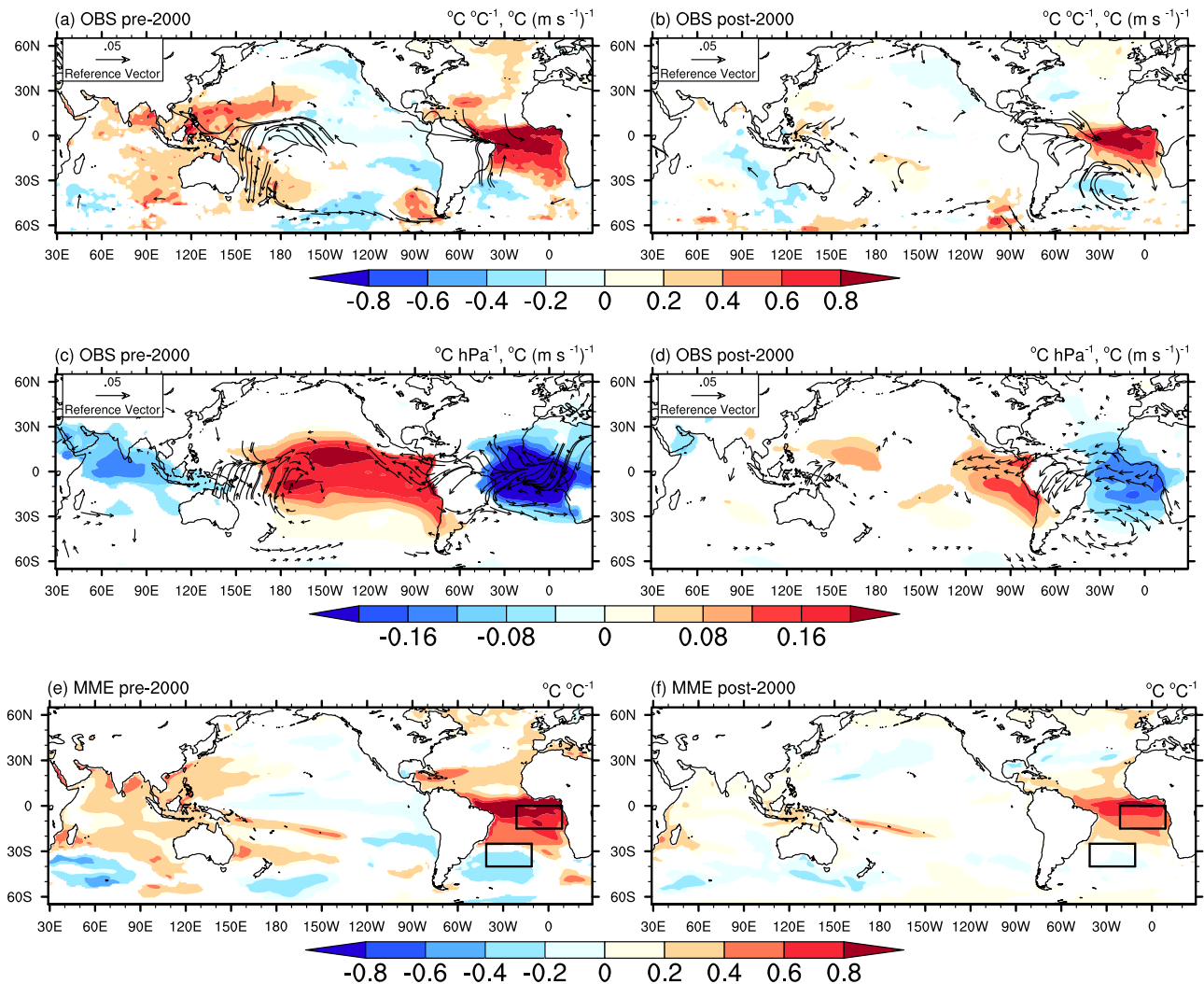


Fig. 2 | Changing relationship between the Atlantic Niño index and various climate fields over the two subperiods. **a, b** regressions of ATL3 index onto the global SSTA (shading) and 850 hPa wind anomalies (vectors) in observations; **c, d** regressions of ATL3 index onto the global sea level pressure (shading) and 200 hPa wind anomalies (vectors) in observations (OBS); **e, f** regressions of ATL3 index onto the global SSTA at the 2-month lead in the multi-model ensemble mean

(MME) predictions. **a, c, e** show results pre-2000; **b, d, f** show results post-2000. Only regressions with significance level of $p < 0.05$ are plotted. Black boxes in **(e, f)** indicate the northeastern pole (NEP) and southwestern pole (SWP) of the South Atlantic Ocean Dipole (SAOD). Wind anomalies are missing in **(e, f)** since wind data are not available from the NMME.

correlations (Supplementary Fig. 3). As previously discussed, the SAOD may also play a role in the prediction skill decline. Therefore, we contrast the Atlantic Niño prediction skills against ENSO-SAOD correlations in Fig. 3. It turns out that the declined prediction skills correlate significantly with the ENSO-SAOD correlations, with less negative ENSO-SAOD relationships leading to lower Atlantic Niño prediction skills. The correlation between Atlantic Niño prediction skills and ENSO-SAOD correlations is -0.64 at the 0-month lead and -0.84 at the 2-month and 3-month lead times, indicating a more important impact of the ENSO-SAOD relationship at these lead times.

To demonstrate how the South Atlantic SSTA is associated with ENSO over the two subperiods, the observed SSTA is regressed onto the observed Niño3.4 index (Fig. 4). Pre-2000, the Pacific Niño leads to the enhanced easterlies over the western equatorial Atlantic, which can deepen thermocline and trigger the cooling over the eastern equatorial Atlantic⁵³. The cooling over the east can form an inter-basin SSTA gradient with the warming over the tropical Pacific, favoring the coupling feedback and the development of Atlantic Niña events¹⁷. In addition, the Pacific Niño enhances the background southeast trade wind over the NEP (northeast pole of the SAOD) region and the prevailing northwesterly wind over the

SWP region (Fig. 4a). The former enhances the cooling over the NEP region via a couple of processes such as subsidence, evaporation, and equatorward advection, while the latter leads to a warming over the SWP region by sending more warm and moist air from the tropics to the subtropics, which suppresses the evaporation²⁵. As the Pacific Niño decays, the cooling over the ATL3 and NEP regions weakens (Fig. 4c, e), but the SSTAs and wind anomalies over the NEP and SWP regions can sustain for more than 6 months, reflecting the stronger negative ENSO-SAOD relationship pre-2000. Post-2000, the Pacific Niño leads to the enhanced easterlies over the western equatorial Atlantic as well (Fig. 4b). However, the easterlies over the western equatorial Atlantic do not lead to an obvious cooling over the east, which could be related to the northerly wind anomalies over the NEP regions, as the cross-equatorial winds can modulate upwelling patterns and cause anomalous SST⁵⁴. The northerly wind anomalies over the NEP region are present for more than 6 months as the Pacific Niño decays (Fig. 4f), which can weaken the background southeast trade wind and curb the cooling over the region, explaining the weak ENSO-SAOD relationship post-2000. Note that there appears to be stronger SST anomalies in the south Atlantic post-2000, although the ENSO influence on the SAOD decreases, which is beyond the scope of this study but deserves further attention.

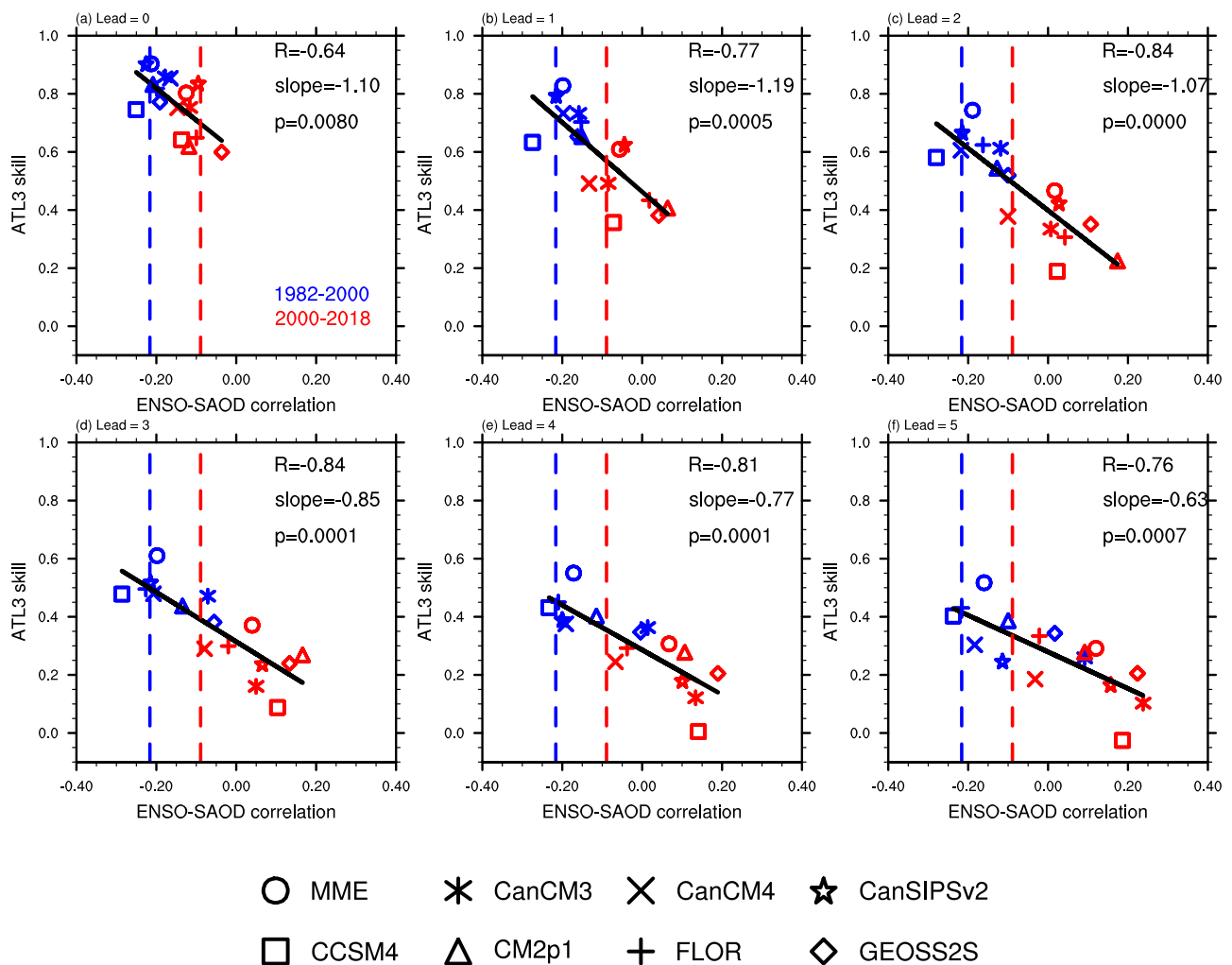


Fig. 3 | Relationship between the Atlantic Niño prediction skill and ENSO-SAOD correlation. Scatter plots of ATL3 prediction skills against ENSO-SAOD correlations over the two subperiods for predictions at **a** 0, **b** 1, **c** 2, **d** 3, **e** 4, **f** 5 lead

months. Blue and red markers indicate prediction skills pre- and post-2000, respectively. Blue and red dashed lines indicate the observed ENSO-ATL3 correlations pre- and post-2000, respectively.

Previous studies have shown that both the remote influence and local oceanic conditions are important for the development of Atlantic Niño^{13,53}. The SSTa gradient between the equatorial Pacific and Atlantic favors the coupling feedbacks and thus the persistence of Atlantic Niño⁴⁷, and may explain the higher Atlantic Niño prediction skill pre-2000. In short, the more negative ENSO-SAOD relationship could be the intrinsic reason to have the higher Atlantic Niño prediction skill pre-2000, and the less negative ENSO-SAOD relationship could lead to the lower Atlantic Niño prediction skill post-2000.

Model deficiency responsible for the decline in Atlantic Niño prediction skill

Although the ENSO-SAOD correlation can explain a large part of the Atlantic Niño prediction skill, model deficiency can give rise to the declined Atlantic Niño prediction skill as well. Figure 2f has indicated that the models may not well capture the enhanced ATL3-SWP relationship. Supplementary Fig. 4 further shows regressions of ATL3 time series onto the South Atlantic SSTa for OBS and the MME predictions at different lead months. Pre-2000, the MME can well capture the observed relationship between the Atlantic Niño and the SWP SSTa, and it changes little as lead time increases. Post-2000, however, MME can basically capture the observed relationship only at 0-month lead, but fails to capture the relationship as lead time increases. It indicates that the dynamical predictions of MME cannot well

reflect the relationship between the ATL3 and SWP at the long leads post-2000.

To determine the extent to which the SWP contributes to the prediction skill of Atlantic Niño, Supplementary Fig. 5 shows results of statistical predictions based on linear regressions as described by Eq. (1). It shows that when the ATL3 index is the only predictor, the prediction skill is clearly higher pre-2000 than that post-2000. When the SWP index is used together with the ATL3 index as the dual predictors, the prediction skills over the two subperiods become comparable, suggesting the complementary role of SWP to the prediction skill decline post-2000. The prediction skill over the second subperiod even exceeds that over the first subperiod at 4- and 5-lead month. Additionally, the Indian Dipole Mode Index⁵⁵, and North Tropical Atlantic Index⁹ can contribute to the prediction skill over the first subperiod, consistent with previous studies^{22,23,35}, but no apparent increase in prediction skill is obtained post-2000. These results reveal that the SWP SSTa contributes to a substantial proportion of the Atlantic Niño predictability post-2000. Therefore, it is very likely that the misrepresentation of ATL3-SWP correlation may be responsible for the much more declined MME prediction skill.

As we try to show a relationship between the change of Atlantic Niño prediction skill and the change of ATL3-SWP correlation, it is found that models cannot well capture the observed ATL3-SWP correlation post-2000 (Supplementary Fig. 6). The negative ATL3-SWP correlation is weakened in

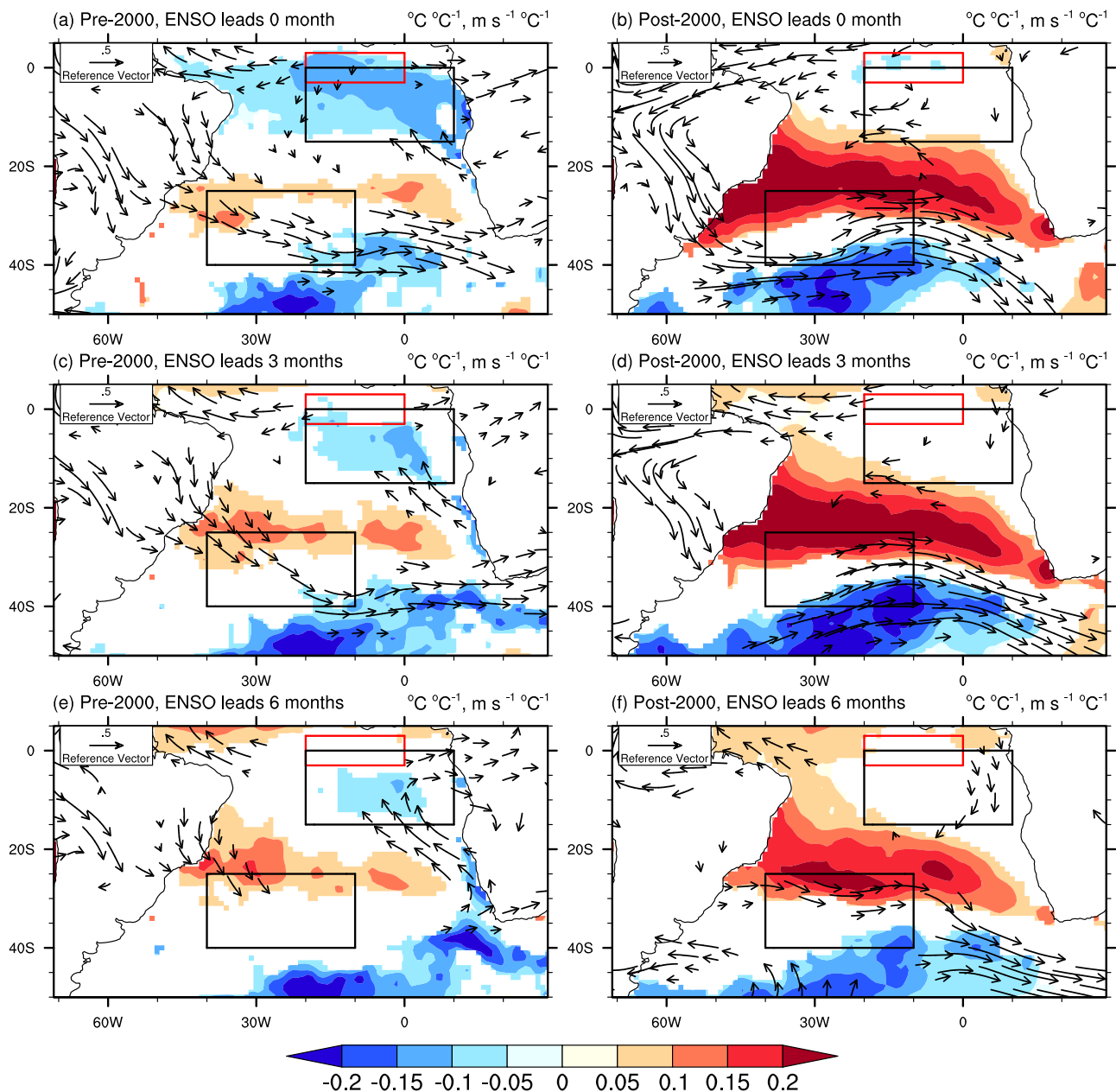


Fig. 4 | Regressions of the Niño3.4 index against the South Atlantic SSTA over the two subperiods in observations. a, b simultaneous regressions of Niño3.4 index against the SSTA and 850hPa wind anomalies. **c, d** same as (a, b), but with the Niño3.4 index leading by 3 months; **e, f** same as (a, b), but with the Niño3.4 index

leading by 6 months; Only regressions with significance level of $p < 0.05$ are plotted. Black boxes indicate the northeastern pole and southwestern pole of the South Atlantic Ocean Dipole. Red box indicates the ATL3 region.

most models, while we know that it is strengthened in OBS (Supplementary Figs. 4 and 6, and Fig. 2). This may explain why the Atlantic Niño prediction skill declines more significant than the persistence. Specifically, OBS shows that the weakened ENSO-SAOD relationship corresponds to the enhanced ATL3-SWP correlation post-2000. The former leads to part of the decline in prediction skill, but the latter can add additional prediction skill to the Atlantic Niño post-2000. As the NMME models fail to faithfully capture the ATL3-SWP correlation post-2000 (Supplementary Figs. 4 and 6), it makes sense that the NMME models show the significant prediction skill decline over the time period. That being said, model experiments should be conducted to verify this idea.

Conclusions

This study aimed to answer how the Atlantic Niño prediction skill would vary as a result of the weakening Atlantic Niño since 2000. By assessing

the NMME hindcasts, this study revealed a significant decline in the Atlantic Niño prediction skill post-2000 that cannot be simply explained by changes in persistence. It was found that the significant decline in Atlantic Niño prediction skill in the NMME relates not only to predictability, but also to deficiencies in dynamical predictions. Further analysis indicated that the changing ENSO-SAOD relationship is the intrinsic reason responsible for the decreased Atlantic Niño persistence, and that the misrepresentation of ATL3-SWP correlation is responsible for the much more declined MME prediction skill. This is because the weakened ENSO-SAOD relationship corresponds to the enhanced ATL3-SWP correlation post-2000. The former leads to part of the decline in the prediction skill, but the latter can add additional prediction skill to the ATL3 SSTA post-2000. That the NMME models fail to faithfully capture the ATL3-SWP correlation post-2000 leads to the significant prediction skill decline.

Previous studies have reported what may lead to the climatic regime shift around 2000 and how the climatic regime shift could lead to changes in ENSO teleconnections. For example, the Atlantic multidecadal oscillation could modulate the Atlantic Niño variability⁵⁰, and the relationship between ENSO and the SSTA over the NEP region may be associated with the Pacific decadal oscillation⁵¹. However, the primary driver of the climate regime shift is beyond the scope of this study as most necessary data are unavailable from the NMME models. Given the various model constructions and initialization schemes included in the NMME predictions, results of this study could suggest a common deficiency in current climate models and prediction systems. By resolving this, it is expected that the dramatic decline in Atlantic Niño prediction skill would be mitigated.

Methods

Model data

The NMME is an ensemble of predictions provided by a number of state-of-the-art climate models from various U.S. and Canadian modeling centers. The NMME is broadly evaluated, conveniently accessible, and widely considered among the most sophisticated predictions available^{32,33}. All models covering the period from 1982 to 2018 were adopted in this study except NCAR CCSM3 and NCEP CFSv2, as both of them show a false increase in Atlantic Niño variability and a low prediction skill. The ensemble mean of each model was used to form a seven-member multi-model ensemble. Supplementary Table 1 provides a brief description of these models

Observational data

Observational data used in this study were the sea surface temperature data from HadISST⁴² and ERSST.v5 datasets⁴³. The wind and sea level pressure data were from NCEP/DOE reanalysis products⁵⁶. All data were interpolated onto a uniform grid of $1^\circ \times 1^\circ$.

Defined indices

The Atlantic Niño has the primary variability peak in JJA, but it can also have a secondary peak in the boreal winter, which is called Atlantic Niño II⁵⁷. Therefore, the current study examines the prediction skill of SST anomalies in the equatorial Atlantic across all calendar months. The Niño3.4 and ATL3 indices are defined as the area-averaged SSTAs over the Niño3.4 (5°S – 5°N , 120° – 170°W) and Atlantic 3 (3°S – 3°N and 20°W – 0°)⁴¹ regions, respectively. The SAOD is defined as the difference between the area-averaged SSTA over its NEP (0° – 15°S , 10°E – 20°W) and SWP (25° – 40°S , 10° – 40°W) according to previous studies^{24,25}. To show changes of Atlantic Niño prediction skill, the studying time period was separated into two subperiods following the previous study³⁶, i.e., 1982–2000 and 2000–2018. The climatology and linear trend were removed for each subperiod separately. The prediction skill was evaluated via the ACC. The persistence ACC was calculated as the autocorrelation of the observed ATL3 index as a function of time lag. The 0-month lead time refers to as one-month integration of prediction from the initial condition. The DMI is defined as the difference in SSTA between the tropical western Indian Ocean (50°E – 70°E , 10°S – 10°N) and the tropical south-eastern Indian Ocean (90°E – 110°E , 10°S – 0°)⁵⁵. The NTA index is defined as the area-averaged SSTAs over the north tropical Atlantic region (80°W – 20°E , 0°N – 15°N)⁹.

The statistical model

To explore the impacts of different factors on prediction skill of the Atlantic Niño, a statistical prediction based on linear regression and leave-one-out cross-validation was established following the previous study⁹. The predictors included climate indices such as the ATL3, Niño3.4, Indian Dipole Mode Index⁵⁵, and North Tropical Atlantic Index⁹ at different leading months, whereas the predictand was the ATL3 index. The regression equation was as follows,

$$y = a + \sum_{i=0}^n b_i x_{li}, \quad l = 0, \dots, 5 \quad (1)$$

where y indicated the ATL3 index, x the index of predictors, l the leading months, i the i -th predictor, a the intercept, and b the regression coefficients. All data over the examined time period, excluding the observed value at the target month and the initial value at the start month, were used to establish the regression models. Statistical prediction was conducted across the two subperiods using different combinations of predictors.

Data availability

The NMME data (<http://iridl.ldeo.columbia.edu/SOURCES/.Models/.NMME/>), HadISST (<https://www.metoffice.gov.uk/hadobs/hadisst/>), ERSSTv5 (<https://www.ncdc.noaa.gov/access/metadata/landing-page/bin/iso?id=gov.noaa.ncdc:C00927>), and NCEP/DOE reanalysis data (<https://www.psl.noaa.gov/data/gridded/data.ncep.reanalysis2.html>) are all available from public repositories.

Code availability

We use basic statistics packages and plotting methods in the NCL software for the analysis.

Received: 2 January 2024; Accepted: 12 September 2024;

Published online: 20 September 2024

References

- Lübbecke, J. F. et al. Equatorial Atlantic variability—Modes, mechanisms, and global teleconnections. *WIREs Clim. Change* **9**, e527 (2018).
- Liu, S. et al. Role of the Maritime Continent in the remote influence of Atlantic Niño on the Pacific. *Nat. Commun.* **14**, 3327 (2023).
- Zhang, L. et al. Emergence of the Central Atlantic Niño. *Sci. Adv.* **9**, eadi5507 (2023).
- Chen, Y. Atlantic Niño induced sea surface salinity variability as observed from the satellite. *Environ. Res. Lett.* **19**, 024027 (2024).
- Keenlyside, N. S. & Latif, M. Understanding equatorial Atlantic interannual variability. *J. Clim.* **20**, 131–142 (2007).
- Lübbecke, J. & McPhaden, M. J. A comparative stability analysis of Atlantic and Pacific Niño mode. *J. Clim.* **26**, 5965–5980 (2013).
- Rodríguez-Fonseca, B. et al. Are Atlantic Niños enhancing Pacific ENSO events in recent decades? *Geophys. Res. Lett.* **36**, L20705 (2009).
- Ding, H., Keenlyside, N. S. & Latif, M. Impact of the Equatorial Atlantic on the El Niño Southern Oscillation. *Clim. Dyn.* **38**, 1965–1972 (2012).
- Ham, Y.-G., Kug, J.-S. & Park, J.-Y. Two distinct roles of Atlantic SSTs in ENSO variability: North Tropical Atlantic SST and Atlantic Niño. *Geophys. Res. Lett.* **40**, 4012–4017 (2013).
- Keenlyside, N. S., Ding, H. & Latif, M. Potential of equatorial Atlantic variability to enhance El Niño prediction. *Geophys. Res. Lett.* **40**, 2278–2283 (2013).
- Exarchou, E. et al. Impact of equatorial Atlantic variability on ENSO predictive skill. *Nat. Commun.* **12**, 1612 (2021).
- Zhao, Y., Jin, Y., Capotondi, A., Li, J. & Sun, D. The role of tropical Atlantic in ENSO predictability barrier. *Geophys. Res. Lett.* **50**, e2022GL101853 (2023).
- Chang, P., Fang, Y., Saravanan, R., Ji, L. & Seidel, H. The cause of the fragile relationship between the Pacific El Niño and the Atlantic Niño. *Nature* **443**, 324–328 (2006).
- Richter, I. et al. Multiple causes of interannual sea surface temperature variability in the equatorial Atlantic Ocean. *Nat. Geosci.* **6**, 43–47 (2013).
- Tokinaga, H., Richter, I. & Kosaka, Y. ENSO influence on the Atlantic Niño, revisited: multi-year versus single-year ENSO events. *J. Clim.* **32**, 4585–4600 (2019).
- Jouanno, J., Hernandez, O. & Sanchez-Gomez, E. Equatorial Atlantic interannual variability and its relation to dynamic and thermodynamic processes. *Earth Syst. Dyn.* **8**, 1061–1069 (2017).

17. Nnamchi, H. C. et al. Thermodynamic controls of the Atlantic Niño. *Nat. Commun.* <https://doi.org/10.1038/ncomms9895> (2015).
18. Nnamchi, H. C. et al. Diabatic heating governs the seasonality of the Atlantic Niño. *Nat. Commun.* **12**, 376 (2021).
19. Chiang, J. C. H. & Vimont, D. J. Analogous Pacific and Atlantic Meridional Modes of Tropical Atmosphere–Ocean Variability. *J. Clim.* **17**, 4143–4158 (2004).
20. Xie, S.-P., & Carton, J. A. Tropical Atlantic variability: Patterns, mechanisms, and impacts. In *Earth's Climate: The Ocean–Atmosphere Interaction Geophysics Monograph Series*, Vol. 147 (eds Wang, C., Xie, S.-P. & Carton J. A.) 121–142 (AGU, Washington, DC, 2004).
21. Lübbecke, J. F., Böning, C. W., Keenlyside, N. S. & Xie, S.-P. On the connection between Benguela and equatorial Atlantic Niños and the role of the South Atlantic Anticyclone. *J. Geophys. Res.* **115**, C09015 (2010).
22. Song, Q., Tang, Y. & Aiki, H. Dual wave energy sources for the Atlantic Niño events identified by wave energy flux in case studies. *J. Geophys. Res. Oceans* **128**, e2023JC019972 (2023).
23. Zhang, L. & Han, W. Indian Ocean Dipole leads to Atlantic Niño. *Nat. Commun.* **12**, 5952 (2021).
24. Nnamchi, H. C., Li, J. & Anyadike, R. N. C. Does a dipole mode really exist in the South Atlantic Ocean? *J. Geophys. Res.* **116**, D15104 (2011).
25. Nnamchi, H. C. et al. An equatorial–extratropical dipole structure of the Atlantic Niño. *J. Clim.* **29**, 7295–7311 (2016).
26. Stockdale, T. N., Balmaseda, M. A. & Vidard, A. Tropical Atlantic SST prediction with coupled ocean–atmosphere GCMs. *J. Clim.* **19**, 6047–6061 (2006).
27. Dippe, T., Lübbecke, J. F. & Greatbatch, R. J. A comparison of the Atlantic and Pacific Bjerknes feedbacks: seasonality, symmetry, and stationarity. *J. Geophys. Res. Oceans* **124**, 2374–2403 (2019).
28. Foltz, G. R., coauthors. The Tropical Atlantic Observing System. *Front. Mar. Sci.* **6**, 206 (2019).
29. Li, X. et al. Monthly to seasonal prediction of tropical Atlantic sea surface temperature with statistical models constructed from observations and data from the Kiel Climate Model. *Clim. Dyn.* **54**, 1829–1850 (2020).
30. Counillon, F. et al. Relating model bias and prediction skill in the equatorial Atlantic. *Clim. Dyn.* **56**, 2617–2630 (2021).
31. Wang, R., Chen, L., Li, T. & Luo, J.-J. Atlantic Niño/Niña prediction skills in NMME models. *Atmosphere* **12**, 803 (2021).
32. Kirtman, Coauthors. The North American Multimodel Ensemble: Phase-1 seasonal-to-interannual prediction; phase-2 toward developing intraseasonal prediction. *Bull. Am. Meteor. Soc.* **95**, 585–601 (2014).
33. Becker, E. J., Kirtman, B. P., L'Heureux, M., Muñoz, Á. G. & Pegion, K. A Decade of the North American Multimodel Ensemble (NMME): research, application, and future directions. *Bull. Am. Meteorol. Soc.* **103**, E973–E995 (2022).
34. Li, X., Tan, W., Hu, Z.-Z. & Johnson, N. C. Evolution and prediction of two extremely strong Atlantic Niños in 2019–2021: Impact of Benguela warming. *Geophys. Res. Lett.* **50**, e2023GL104215 (2023).
35. Liu, A. et al. Impact of Indian Ocean Dipole on Atlantic Niño predictive skill. *Environ. Res. Lett.* **18**, 074015 (2023).
36. Prigent, A. et al. Weakened SST variability in the tropical Atlantic Ocean since 2000. *Clim. Dyn.* **54**, 2731–2744 (2020).
37. Crespo, L. R. et al. Weakening of the Atlantic Niño variability under global warming. *Nat. Clim. Chang.* **12**, 822–827 (2022).
38. Yang, Y. et al. Suppressed Atlantic Niño/Niña variability under greenhouse warming. *Nat. Clim. Chang.* **12**, 814–821 (2022).
39. Richter, I., Tokinaga, H. & Okumura, Y. M. The extraordinary equatorial Atlantic warming in late 2019. *Geophys. Res. Lett.* **49**, e2021GL095918 (2022).
40. Lee, S.-K. et al. On the genesis of the 2021 Atlantic Niño. *Geophys. Res. Lett.* **50**, e2023GL104452 (2023).
41. Zebiak, S. E. Air–sea interaction in the equatorial Atlantic region. *J. Clim.* **6**, 1567–1586 (1993).
42. Rayner, N. A. et al. Global analyses of sea surface temperature, sea ice, and night marine air temperature since the late nineteenth century. *J. Geophys. Res.* **108**, 4407 (2003).
43. Huang, B. et al. Extended Reconstructed Sea Surface Temperature version 5 (ERSSTv5), Upgrades, validations, and intercomparisons. *J. Climate* <https://doi.org/10.1175/JCLI-D-16-0836.1> (2017).
44. Tang, Y., Kleeman, R., Moore, A. M., Weaver, A. & Vialard, J. The use of ocean reanalysis products to initialize ENSO predictions. *Geophys. Res. Lett.* **30**, 1694 (2003).
45. Balmaseda, M. A. et al. Ocean initialization for seasonal forecasts. *Oceanography* **22**, 154–159 (2009).
46. Chen, Y., Shen, Z., Tang, Y. & Song, X. Ocean data assimilation for the initialization of seasonal prediction with the Community Earth System Model. *Ocean Model.* **183**, 102194 (2023).
47. Wang, C. An overlooked feature of tropical climate: Inter-Pacific–Atlantic variability. *Geophys. Res. Lett.* **33**, L12702 (2006).
48. Richter, I. et al. On the triggering of Benguela Niños: remote equatorial versus local influences. *Geophys. Res. Lett.* **37**, L20604 (2010).
49. Martín-Rey, M. et al. On the Atlantic–Pacific Niños connection: a multidecadal modulated mode. *Clim. Dyn.* **43**, 3163–3178 (2014).
50. Martín-Rey, M., Polo, I., Rodríguez-Fonseca, B., Losada, T. & Lazar, A. Is there evidence of changes in tropical Atlantic variability modes under AMO phases in the observational record? *J. Clim.* **31**, 515–536 (2018).
51. Zhang, S., Liu, Y., Dong, B. & Sheng, C. Decadal modulation of the relationship between tropical southern Atlantic SST and subsequent ENSO by Pacific decadal oscillation. *Geophys. Res. Lett.* **50**, e2023GL104878 (2023).
52. Losada, T. & Rodríguez-Fonseca, B. Tropical atmospheric response to decadal changes in the Atlantic Equatorial Mode. *Clim. Dyn.* **47**, 1211–1224 (2016).
53. Illig, S., Gushchina, D., Dewitte, B., Ayoub, N. & du Penhoat, Y. The 1996 equatorial atlantic warm event: origin and mechanisms. *Geophys. Res. Lett.* **33**, L09701 (2006).
54. Philander, S. G. H. & Pacanowski, R. C. The oceanic response to cross-equatorial winds (with application to coastal upwelling in low latitudes). *Tellus* **33**, 201–210 (1981).
55. Saji, N. H., Goswami, B. N., Vinayachandran, P. N. & Yamagata, T. A dipole mode in the tropical Indian ocean. *Nature* **401**, 360–363 (1999).
56. Kanamitsu, M. et al. NCEP–DOE AMIP-II Reanalysis (R-2). *Bull. Am. Meteorol. Soc.* **83**, 1631–1644 (2002).
57. Okumura, Y. & Xie, S.-P. Some overlooked features of tropical Atlantic climate leading to a new Niño-like phenomenon. *J. Clim.* **19**, 5859–5874 (2006).

Acknowledgements

The authors thank the three anonymous reviewers for their constructive comments. This work is supported by the National Natural Science Foundation of China (42130409; 42176028; 523035611) and the high-level personal project of Jiangsu province JSSCRC2021492.

Author contributions

Yihao Chen, Youmin Tang, and Qingyang Song contributed to the conceptualization. Yihao Chen and Xiaoqin Yan performed the analysis. Yihao Chen plotted the figures and wrote the first draft of the manuscript. Yihao Chen, Xiaoqin Yan, Youmin Tang, and Qingyang Song contributed to reviewing and editing of the manuscript. Xiaoqin Yan, Youmin Tang, Qingyang Song, Yanling Wu, and Zheqi Shen contributed to interpreting the results, discussion of the mechanisms, and improvement of this paper.

Competing interests

The authors declare no competing interests.

Additional information

Supplementary information The online version contains supplementary material available at

<https://doi.org/10.1038/s43247-024-01693-0>.

Correspondence and requests for materials should be addressed to Xiaoqin Yan or Youmin Tang.

Peer review information *Communications Earth & Environment* thanks Lin Chen and the other, anonymous, reviewer(s) for their contribution to the peer review of this work. Primary Handling Editors: Heike Langenberg, Alienor Lavergne. A peer review file is available.

Reprints and permissions information is available at <http://www.nature.com/reprints>

Publisher's note Springer Nature remains neutral with regard to jurisdictional claims in published maps and institutional affiliations.

Open Access This article is licensed under a Creative Commons Attribution-NonCommercial-NoDerivatives 4.0 International License, which permits any non-commercial use, sharing, distribution and reproduction in any medium or format, as long as you give appropriate credit to the original author(s) and the source, provide a link to the Creative Commons licence, and indicate if you modified the licensed material. You do not have permission under this licence to share adapted material derived from this article or parts of it. The images or other third party material in this article are included in the article's Creative Commons licence, unless indicated otherwise in a credit line to the material. If material is not included in the article's Creative Commons licence and your intended use is not permitted by statutory regulation or exceeds the permitted use, you will need to obtain permission directly from the copyright holder. To view a copy of this licence, visit <http://creativecommons.org/licenses/by-nc-nd/4.0/>.

© The Author(s) 2024